



Research Article

Next-Generation Nutrient Delivery: Physicochemical Insights into Multicomponent Liposomes

Jie Chen^{1,2}, Leila Dehabadi¹, Amandio Vieira³, Yuan-Chun Ma^{1,2*}, Lee Wilson^{4**}

¹Dr. Ma's Laboratories Inc., Unit 4, 8118 North Fraser Way, Burnaby, BC V5J 0E5, Canada

²North American Institute of Medicinal Plants, 19062 34A Ave, Surrey, BC V3S 0L5, Canada

³Department of Biomedical Physiology and Kinesiology, Simon Fraser University, 8888 University Drive, Burnaby, BC V5A 1S6, Canada

⁴Department of Chemistry, University of Saskatchewan, 110 Science Place, Saskatoon, SK S7N 5C9, Canada

*Corresponding author: ycma@dml-labs.com; Tel.: +16044396089

**Corresponding author: lee.wilson@usask.ca; Tel.: +13069662961

Abstract: Innovative food-grade lipid-based formulations incorporating multicomponent nutrients: vitamin C with vitamin D3 and vitamin D3 with calcium, were developed. Morphological characteristics, particle size, and physical stability were assessed using transmission electron microscopy (TEM), dynamic light scattering (DLS), and zeta potential analysis. High-Performance Liquid Chromatography (HPLC) was used to quantify vitamin C and vitamin D3 directly, while calcium was measured indirectly via its chelated amino acid complex. TEM imaging results confirmed the formation of spherical unilamellar vesicles across all formulations. DLS analysis revealed an average particle size of 168.3 nm with a zeta potential of -22.9 mV for the vitamin C plus D3 formulation and 329.3 nm with a zeta potential of -5.2 mV for the calcium plus D3 formulation. Encapsulation efficiency (EE) was determined to be approximately 50% for vitamin C and >90% for vitamin D3. Stability assessments over a six-month period at 4 °C and 25 °C indicated high retention rates for calcium (>98%) and vitamin C (>92%), whereas vitamin D3 retention ranged between 70% and 87% depending on storage temperature. Calcium maintained complete stability under simulated gastrointestinal digestion, while vitamin D3 retained an encapsulation efficiency exceeding 30%. These findings demonstrate that liposomal encapsulation effectively accommodates nutrients with differing hydrophilic and lipophilic properties, yielding homogeneous, stable formulations with enhanced oral bioavailability.

Keywords: Liposomal encapsulation; Multivitamin–Multimineral supplement; Oral bioavailability; Simulated digestion; Quantitative analysis

1. Introduction

The spherical vesicular structure of liposomes is characterized by the formation of one or more concentric phospholipid bilayers (Akbarzadeh et al., 2013). This unique structure enables the encapsulation of both fat-soluble and water-soluble substances. Hydrophobic molecules can reside within the lipid bilayer, nestled among the fatty acid tails, while hydrophilic substances are enclosed within the aqueous core of the sphere, adjacent to the hydrophilic phospholipid heads (Shade, 2016). Liposomes serve as highly efficient supramolecular nanocarriers in drug delivery and related imaging applications, which stem from their capacity to encapsulate and transport various molecular cargo with diverse characteristics (Wibowo et al., 2021). The pharmacokinetics of liposome absorption in the intestine can modify the typical absorption profile of active compounds in aqueous environments upon oral administration. This leads to a potentially enhanced distribution and effective encapsulation of dietary supplements or pharmaceuticals (Noble et al., 2014; Deshpande et al., 2013; Barenholz, 2012).

Notably, liposome formulations that exhibit inadequate pharmacokinetic properties when

administered independently have obtained clinical approval for drug delivery (Noble et al., 2014; Deshpande et al., 2013; Barenholz, 2012). A key functional attribute of liposomes is their ability to encapsulate, protect, and transport substances, which offers significant potential for delivering inorganic minerals, such as calcium phosphates, which are relevant to biomedical and dental applications (Shade, 2016). The development of liposomal delivery systems, in which nutrients are enclosed within liposomes, alters the physicochemical properties of the encapsulated compounds, which may improve their absorption and bioavailability (Shade, 2016). Liposomal packaging may protect contents from a harsh gastrointestinal environment due to the supramolecular barrier effect and enhanced cellular absorption arising from interactions between the liposome bilayer and cell membrane components. Using liposome carriers for drug administration may confer key advantages over conventional approaches, including improved stability, biocompatibility, and versatility (Daraee et al., 2016; Akbarzadeh et al., 2013). The dispersion profile of a substance that usually undergoes slow or controlled absorption can be altered when bioactive species are enclosed within a liposome, as seen with vitamin C (Mankan et al., 2025; Kraft et al., 2014).

The current study aimed to acquire further knowledge regarding the function of multi-components (e.g., vitamin C plus vitamin D3) in the delivery of a liposomal formulation. This aim contrasts with the properties of previously reported single-component liposome systems (Chen et al., 2022). The underlying hypothesis of this study is that liposomal vitamin C plus D3 would outperform the respective individual liposomal formulations in terms of stability and encapsulation efficiency, which supports the concept of improved bioavailability (Davis et al., 2016). As a point of reference, we have quantified the levels of lipid-based vitamin C plus vitamin D3, calcium aspartate plus vitamin D3, and calcium aspartate as a single component following a simulated digestive system environment.

Phosphate-loaded liposomes have been engineered to reproduce the early processes of matrix vesicle-mediated mineralization (Ghadami and Dellinger, 2023). These vesicles are formed from phosphatidylcholine, diacetyl phosphate, and cholesterol, which become permeable to external Ca^{2+} using a calcium ionophore (Skrinda-Melne et al., 2024; Huang et al., 2024). Calcium influx inside the liposome instigates apatite mineral nucleation. As hydroxyapatite (HA) crystals grow, they eventually disrupt the liposomal membrane and protrude outward, creating nucleation sites in the surrounding medium for further mineral growth. This model provides a well-controlled system to study the physicochemical and molecular mechanisms of matrix vesicle calcification (Dangkoub et al., 2024). In this context, we describe the procedure for preparing calcium aspartate-loaded liposomes and detail the parameters that affect calcium ion (Ca^{2+}) encapsulation and stability.

Multivitamin and mineral supplements (MVMs) are among the most widely consumed dietary supplements that have been used as part of routine nutritional support for decades (Tinsley et al., 2022; AlSawaftah et al., 2021). To guarantee the accessibility of essential nutrients, recommendations from both the American Medical Association (US Preventive Services Task Force et al., 2022) and the National Institutes of Health (National Institutes of Health Office of Dietary Supplements) encourage individuals to incorporate a daily multivitamin supplementation into their nutrition routine. According to a Delphi analysis conducted by an international panel of nutrition experts, the regular daily intake of multivitamin supplements may play a significant role in reducing the risk of micronutrient deficiencies, especially among vulnerable populations (Blumberg et al., 2018). The International Society of Sports Nutrition recommends that athletes and physically active individuals include a multivitamin supplement in their daily regimen, emphasizing the importance of iron supplementation for female athletes to support adequate micronutrient intake during periods of intense training (Kerksick et al., 2018). Daily multivitamin use has become a widespread practice for promoting overall health. This raises the question of whether liposome-coated multivitamin and mineral (MVM) supplements offer enhanced bioavailability of vitamins and minerals compared to conventional, non-liposomal formulations (Sapei et al., 2024). Tinsley et al. reported that MVM supplements encapsulated in

liposomes enhanced iron absorption compared with conventional MVM formulations, although no significant difference was observed in magnesium absorption. To date, this appears to be the only known study specifically evaluating the impact of liposomal encapsulation on the bioavailability of vitamins and minerals within a complete MVM supplement (Tinsley et al., 2022). In accordance with this concept, the goal of the present research is to assess the levels of vitamins and minerals in the body following the oral intake of MVMs that are encapsulated before digestion. This condition is relevant compared with MVMs enclosed within liposomes after the simulated digestive system.

2. Materials and Methods

Sigma-Aldrich (New York, NY, USA) supplied vitamin C (sodium ascorbate, 99.70%) and vitamin D3 (cholecalciferol, 98.50%). BYL Pharmaceuticals Ltd. (Vancouver, BC, Canada) supplied calcium aspartate (calcium assay, 12.02%). Jedwards International, Inc. (Braintree, Chicago, IL, USA) supplied the sunflower lecithin (phosphatidylcholine, 40%). Quadra Chemicals in Delta, BC (Canada) supplied the potassium sorbate (99.50%). EZ Chemicals Inc. in Mississauga, ON (Canada) supplied glycerin (99.90%). All solutions were prepared using 100% olive oil obtained from Kirkland, WA (USA) and distilled water (ELGA LabWater) from Woodridge, IL (USA). VWR International, LLC supplied methanol (UHPLC grade, 99.80%) and acetonitrile (UHPLC grade, 99.99%). EMD Millipore Corporation in Kankakee, Illinois (USA) supplied phosphoric acid (HPLC grade, 85.00% w/w). Ammonia solution (ammonium hydroxide, HPLC grade, 25% w/w) was supplied acquired by from Millipore Sigma in Burlington, MA (USA). All solvents and samples were filtered before injection into the HPLC system using a 0.2 μ m PTFE syringe filter (Pall Corporation, New York, NY, USA).

2.1 Method of Preparation of Liposomal Vitamin C and Vitamin D3

The process was conducted at room temperature (RT; 25 °C) as follows: First, 0.268 g of potassium sorbate (99.50%) was added to 45 mL of purified water. This mixture was stirred until completely dissolved. Subsequently, 22.497 (+5%) g of vitamin C (sodium ascorbate, 99.70%) was introduced into the solution, with 5 % surplus as specified in the sample product formula. Then, 55-mL glycerin (99.90%) was added, which was incorporated into the aqueous media via stirring. The resulting mixture was placed in a blender (Hamilton Beach, Avalon, NJ, USA) and thoroughly mix at a high speed of 3000 rpm. Subsequently, 0.5 (+10%) mg of vitamin D3 (cholecalciferol, 98.50%) was dissolved in 0.3 mL of olive oil (100%). This mixture was added to the previous solution and blended at 3000 rpm for 30 min. Finally, 3.32 g of sunflower lecithin (40%) was added to the aqueous media and blended at 3000 rpm. This process led to the creation of liposome-encapsulated vitamin C plus vitamin D3.

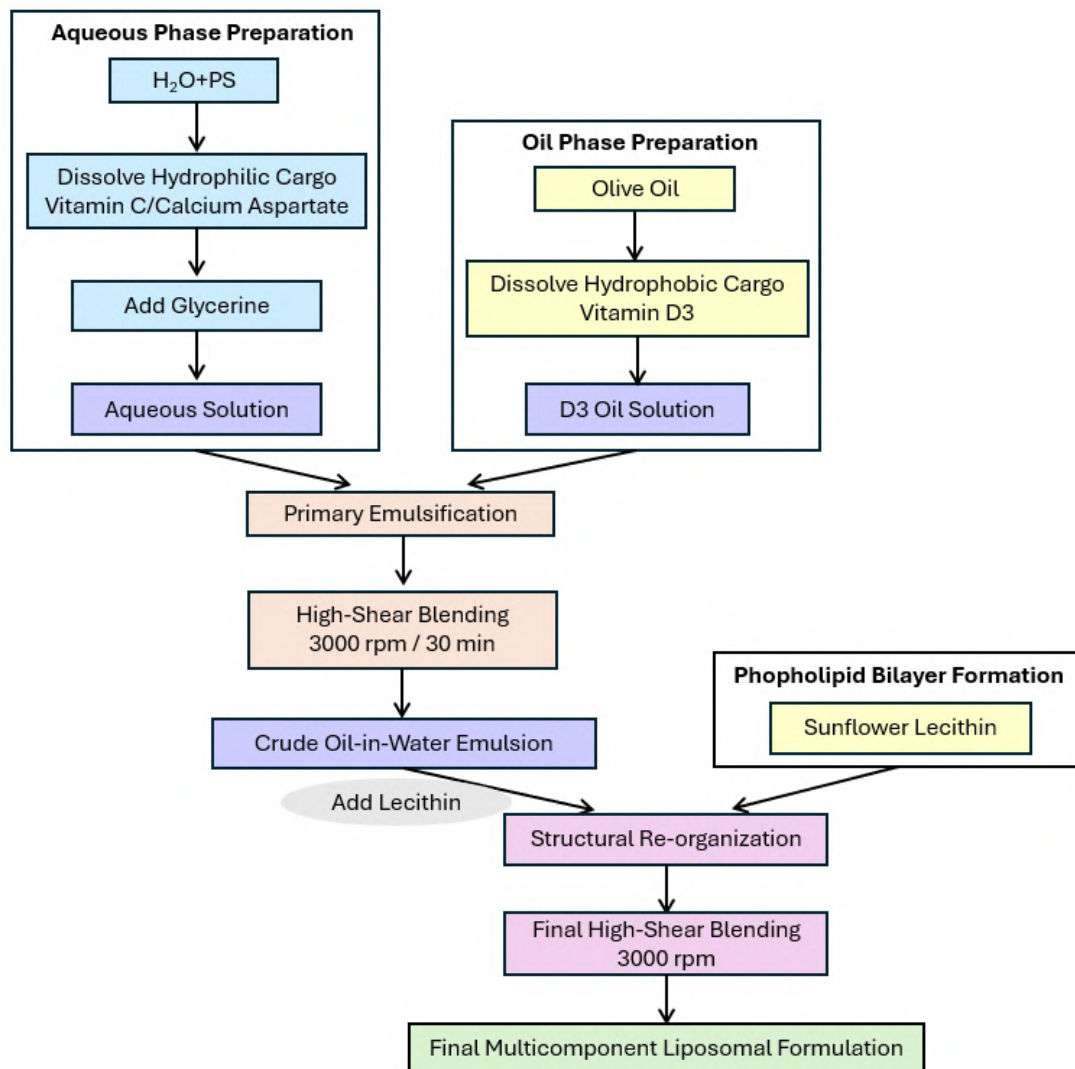
2.2 Preparation of Liposomal Calcium

The procedure was performed at RT following these steps. First, 0.268 g of potassium sorbate (99.50%) was dissolved in 45 mL of purified water until it was completely dissolved to obtain an aqueous solution. Then, 14.45 g calcium aspartate (containing 12.02% calcium) was added and completely dissolved in the solution. Then, 55 mL glycerin (99.90%) was added to the aqueous solution through stirring. The solution was transferred to a blender container, as described in Section 2.1. Finally, 3.32 g of sunflower lecithin (phosphatidylcholine, 40%) was added to the aforementioned solution, and the mixture was blended to achieve liposome-encapsulated calcium.

2.3 Method of Preparation of Liposomal Calcium and Vitamin D3

The following procedure was used to prepare the formulation at room temperature. An initial solution was prepared by solving 0.268 g of potassium sorbate (99.50%) in 45 mL of

filtered water. Then, 10.84 g calcium aspartate (containing 12.02% calcium) was added to the water solution and dissolved. Then, 55 mL of glycerin (99.90%) was added to the previous solution and stirred, followed by thorough mixing at a high speed, as described in Section 2.1. Subsequently, 0.25 (+10%) mg of vitamin D3 (cholecalciferol, 98.50%) was dissolved in 0.3 mL (100.00%) olive oil. The vitamin D3-oil combination was then added to the previously prepared solution and blended for 30 minutes at 3000 rpm. To achieve liposome-encapsulated calcium with vitamin D3, 2.8 g of sunflower lecithin (phosphatidylcholine, 40%) was added to the aqueous solution and mixed thoroughly at 3000 rpm to complete the formulation process.



Scheme 1 Preparative method for the formulation of multicomponent liposomal systems. This schematic illustrates the sequential steps involved in the formulation process, from separate aqueous and oil phases to the final multicomponent liposome, highlighting key mixing, homogenization, and encapsulation stages

2.4 Characterization of vitamin C plus vitamin D3, calcium, and calcium plus vitamin D3 in liposomes

2.4.1 Transmission electron microscopy (TEM) analysis

Negative staining was employed for transmission electron microscopy (TEM) analysis. Briefly, a 5 μ L sample of liposomes was placed on a TEM grid coated with copper-formvar. After allowing it to settle for 2 min, an absorbent tissue was used to absorb the excess fluid. The grid was stained for 20 seconds with 0.5% phosphotungstic acid for 20 s, and any excess

staining was removed. An HT7700 TEM (Hitachi, Tokyo, Japan) operated at an accelerating voltage of 80 kV was used for imaging.

2.4.2 Analysis of PSD and zeta potential

The particle size and zeta potential of the liposomes were determined using a Malvern Zetasizer Nano ZS device (Malvern Instruments Ltd., Malvern, UK). The sample size distribution was measured using DLS, which measures the scattered light at a defined angle ($\theta = 173^\circ$) from particles exposed to a laser beam. An electrophoretic light scattering protocol was employed to calculate the zeta potential, using the Doppler effect (Irawan et al., 2017). The zeta potential charge values were determined through triplicate measurements, with each measurement comprising at least 10 separate runs.

2.4.3 Encapsulation efficiency (EE%) and vitamin loading efficiency (LE%)

The encapsulation efficiency (EE%) of the vitamins in the liposomes was determined using Equation (1) (Vakilinezhad et al., 2018; Afroz et al., 2017; Mohammadi et al., 2014):

$$EE(\%) = \frac{\text{Total Vitamin Content (mg)} - \text{Vitamin Content in Permeated Solution (mg)}}{\text{Total Vitamin Content (mg)}} \times 100 \quad (1)$$

Following ultrafiltration through membranes with a 10 kDa cutoff mass (Pall Corporation, Port Washington, NY, USA) and centrifugation (Nuaire, NU-C200R, Plymouth, MA, USA) at $2500 \times g$ for 20 min at 4°C , the non-encapsulated vitamins in the permeate solution were quantified using UHPLC (Blumberg et al., 2018). The absorbance indicated the non-encapsulated vitamin content, enabling the indirect calculation of the amount of trapped vitamins using Equation (1). The vitamin loading efficiency (LE%) refers to the amount of vitamin that has been encapsulated in hydrated liposomes, according to Equation (2) (Vakilinezhad et al., 2018; Afroz et al., 2017; Jeung, 2016):

$$LE(\%) = \frac{\text{Vitamin Content in Liposomes (mg)}}{\text{Weight of Liposomes (mg)}} \times 100 \quad (2)$$

2.4.4 Instrumentation and chromatographic conditions of the liquid

The UHPLC system comprised flexible pumps, multicolumn thermostats, vial samplers, and a diode array detector (Agilent 1290 Infinity II, Santa Clara, CA, USA). Vitamin C was separated using a Phenomenex Luna C18 column (100 mm \times 3.0 mm, 2.5 μm) from Torrance, CA, USA, employing a gradient elution program at a flow rate of 1.0 mL/min at isothermal conditions (30.0°C). In the UHPLC system, the injection volume was 1 μL , and the mobile phase consisted of 0.1% (v/v) phosphoric acid (A) and acetonitrile (B). The following linear gradient was applied: 0-5 minutes: 50-20% A; 5-10 minutes: 20% A. Following the gradient, the system was re-equilibrated for 5 min before the subsequent run. The vitamin C analyte was detected at a wavelength of 265 nm.

Vitamin D3 separation was accomplished through an isocratic elution process at a flow rate of 0.5 mL/min, while isothermally maintained at 30.0°C . This was performed using a Phenomenex Luna C18 column (100 mm \times 3.0 mm, 2.5 μm). In the UHPLC system, an injection volume of 10 μL was employed, and the mobile phase consisted of 75% acetonitrile (A) and 25% methanol (B). Isocratic elution was completed over a period of 10 min. Vitamin D3 was detected at a wavelength of 280 nm.

L-aspartic acid was separated from calcium L-aspartate using an isocratic elution program at a flow rate of 0.5 mL/min, maintained at 25.0°C . This separation was achieved using a Phenomenex Luna C18 column (100 mm \times 3.0 mm, 2.5 μm) from Torrance, CA, USA. In the UHPLC system, the injection volume was 1 μL , and the mobile phase comprised 60% of 0.004%

(v/v) aqueous ammonium hydroxide (A) and 40% acetonitrile (B). The isocratic elution process was completed within 5 min. L-aspartic acid was detected at a wavelength of 195 nm.

2.4.5 Preparation of samples for ultrahigh-performance liquid chromatography analysis

Samples containing vitamin C and vitamin D3 from the top and bottom of the centrifuge tube were diluted with 100% methanol in a volume ratio of 1:100 (v/v) and sonicated for 30 min before filtering for injection. In a 10 mL volumetric flask, 0.1 mL of liposomal calcium and calcium plus vitamin D3 from the top and bottom regions of the sample tube were diluted with 0.2% (v/v) aqueous ammonium hydroxide and brought to the volume. The samples were sonicated for 30 min before being filtered and injected.

2.4.6 Stability of the Liposomal Formulations

The stability of liposomal formulation was evaluated by calculating the remaining vitamins and minerals in the liposomes during a certain period or at certain conditions using Equation (3) (Mohammadi et al., 2014):

$$\text{Stability}(\%) = \frac{\text{Remaining Amount of Vitamin/Mineral in Liposomes (mg)}}{\text{Initial Amount of Vitamin/Mineral Incorporated in Liposomes (mg)}} \times 100 \quad (3)$$

2.4.7 In vitro digestion system

The samples were digested by successive incubation in simulated gastric fluid (SGF) and then in simulated intestinal fluid (SIF) using a modified in vitro digestion methodology (Frenzel et al., 2015).

The gastric fluid stage. Simulated gastric fluid with a pH adjusted to 2.0 employed HCl (*aq*) and consisted of 58.44 mg/mL of NaCl, 8.8 mg/mL of fresh pepsin, and 20 mL of distilled water. To mimic stomach digestion, 20 mL of liposome sample solution was mixed with 20 mL of SGF in a 50 mL beaker, and the mixture was incubated for 1 hour at 37 °C and swirled for an additional 1 h at 100 rpm.

Small intestinal fluid stage. 30 mL of the gastric digest was combined with 5 mL of SIF containing 3.672 mg/mL KH₂PO₄ and 5.4 mg/mL pancreatin after 1 h of incubation in the SGF. To imitate intestinal digestion, the temperature was set to 37 °C, the pH was raised to 7.5 using 1 M NaOH, and the pH was maintained at 7.0 for the subsequent 2 h of incubation with stirring at 100 rpm.

3. Results and Discussion

As stated in Section 1, a primary objective of this research was to generate a solubilized water and lipid-based co-formulation characterized by homogeneity and stability that contains vitamins plus minerals. The above mentioned formulations were prepared without the use of any hazardous substances or solvents, where we introduced a novel method for quantifying minerals encapsulated within liposomes.

Characterization of the colloidal lipid-based formulation comprising vitamin C, vitamin D, and calcium is presented below using various techniques, including TEM imaging, light scattering, and HPLC. To evaluate the stability of these colloidal formulations, the physicochemical characterization is related to the structure and various parameters, such as particle size, zeta potential, encapsulation efficiency (EE%) of the vitamins/minerals, and vitamin/mineral loading efficiency (LE%) of the liposomes.

3.1 Formulation Optimization

The goal of this work was to create an ideal lipid-based formulation with favorable stability and colloidal uniformity, in line with a prior study (Chen et al., 2022). The ratio of water to glycerin was shown to be essential in the sample preparation procedure. A comparative analysis of samples with varying water-to-glycerin ratios, indicated that the most effective volume ratio for water-to-glycerin was 45:55 (v/v) as the optimized condition. Furthermore, the sequence in which the ingredients were mixed during homogenization had a profound influence on achieving uniformity of the resulting liposome encapsulated liquid (LEL) formulation.

3.2 Morphological Characterization by TEM

TEM was used to obtain microscopy images that detail the size and morphology of the resulting vitamin C plus D3 liposome. As shown in Figure 1(a), the TEM images indicated that the liposomes were in the form of tiny spherical structures. The bilayer liposomes observed in the microscopy images support the notion that the organized lipid structures are liposomal. The TEM results confirmed the successful formation of liposomes across all formulations (Nakhaei et al., 2021). ImageJ software (U.S. National Institute of Health, Bethesda, MD, USA) was employed to analyze the average particle size of the liposomes, which was expected to be near 200 nm for liposomal vitamin C plus vitamin D3 formulation, was calculated. The TEM results also revealed that the microstructure of all liposomal samples exhibited a spherical shape without any adhesion or breakage. This vitamin C or D3 encapsulation did not affect the structural integrity of the liposomes. The liposomes loaded with both vitamin C (VC) and vitamin D3 (VD3) were larger in size than liposomes loaded solely with VC or VD3, respectively (Liu et al., 2020). Figure 1(b) shows the TEM image of the liposome dispersions in the liposomal calcium plus VD3 formulation. In this case, the loaded liposomes exhibited a predominantly spherical and near-spherical shape. The size observed in the micrograph aligns with the average hydrodynamic diameter values obtained through photon correlation spectroscopy, which matches the generated bimodal size distributions (Chaves et al., 2018). Figure 1(c) shows the approximate size of the nanoparticles, which ranged from 100 to 300 nm. These nanoparticles contained calcium L-aspartate and displayed unique characteristics, particularly the tendency to aggregate and form a hierarchical structure (Tinsley et al., 2022).

3.3 Particle size and zeta potential

The surface charge, electrostatic repulsion between adjacent particles, colloidal stability, and entrapment efficiency were all associated with the zeta potential (ζ) (Raval et al., 2019). Liposome properties, such as particle size, rigidity, fluidity, stability, and electrical charge, are heavily influenced by lipid content (Strange et al., 2015). The particle sizes of encapsulated liposomal VC plus VD3 and liposomal calcium plus VD3 were 168.3 and 329.3 nm, respectively, with a zeta potential of -22.9 mV and -5.2 mV, respectively (Figure 1a, 1b). The obtained calcium-loaded liposomes have a wide size variability, with the main size category being fairly large, typically exceeding above 500 nm in diameter (Ko et al., 2023). The particle size of encapsulated liposomal calcium was 606 nm with a zeta potential of -5.0 mV (Figure 1c). The surface charge of nanoparticles is commonly characterized by their ζ -value. The ζ -values signify the electrical charges of particles and are measured from a plane situated just outside the fluid layer associated with the particle. The ζ -values are frequently determined by analyzing the electrophoretic mobility of the particle and reveal linear changes in response to the proportion of ionic lipids integrated into the liposomes. A ζ -value between -30 mV to $+30$ mV is generally considered adequate to promote interparticle repulsion (IPR). In turn, a favorable range of ζ -values contributes to the favorable colloidal stability of particle suspensions (Tenchov et al., 2021).

3.4 Evaluation of Encapsulation Efficiency (EE%) and Loading Efficiency (LE%)

Table 1 lists the encapsulation efficiency (EE%) and loading efficiency (LE%) of liposomal vitamin C plus D3 and liposomal calcium plus vitamin D3. These properties are governed by the liposome composition. The values of EE% and LE% may be influenced by other factors, such as liposome size, type, surface charge, bilayer rigidity, preparation processes, and the physical properties of the vitamins and minerals used. This potential enhancement in liposomal stability could lead to increased physiological bioavailability without compromising the potency of delivered nutrients throughout the digestive tract at the cellular level (Nsairat et al., 2022; Lukawski et al., 2020; Lee, 2020).

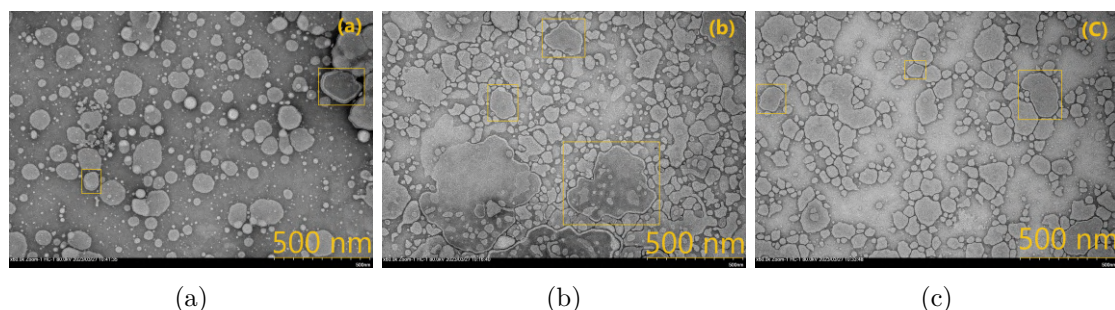


Figure 1 Images obtained from transmission electron microscopy (TEM): (a) liposomal vitamin C plus vitamin D3 with an average diameter (d_{avg}) of 100-200 nm; (b) liposomal calcium plus vitamin D3 with $d_{avg} = 50-800$ nm; and (c) liposomal calcium with $d_{avg} = 100-300$ nm. The square represents a sample of a bilayer (unilamellar) vehicle. The scale bars (bottom right) in panels (a, b, and c) reflect a liposomal size range

Table 1 Encapsulation Efficiency (EE%) and Vitamin Loading Efficiency (LE%) of liposomal vitamin C plus D3 and liposomal calcium plus vitamin D3

Liposomal Formulation	Encapsulation Efficiency (EE%)		Vitamin Loading Efficiency (LE%)	
	Vitamin C	Vitamin D3	Vitamin C	Vitamin D3
Vitamin C plus D3	> 45.0%	> 90.0%	264.3%	0.0133%
Calcium plus Vitamin D3	—	> 85.0%	—	0.0030%

3.5 Determination of Vitamin C and vitamin D3 Potencies in Liposomal vitamin C plus D3

Based on foundational research that reported encapsulation efficiencies (EE%) of approximately 50% for vitamin C and >90% for vitamin D3 utilizing similar liposome preparation protocols (Chen et al., 2022; Maione-Silva et al., 2019; Dalmoro et al., 2019; Vakilinezhad et al., 2018), the concentrations of VC and VD3 in the liposomal formulation of vitamin C plus vitamin D3 were determined using ultrahigh performance liquid chromatography (UHPLC) equipped with a DAD detector, with wavelengths of 265 and 280 nm for VC and VD3, respectively. Table 2 provides the concentration values for VC and VD3 in both the upper and lower regions of the sample tube (cf. inset in Figure 2A. a, b and Figure 2B. a, b). The recovery (%) for vitamin C was 98.8% and 101.6%, whereas that for vitamin D3 was 102.5% and 95.3%. These results indicate that the sample was homogeneous and did not exhibit any phase separation. According to the regulations for Natural Health Products of Health Canada, a variation of up to 20% in composition is permissible for the industrial production of such vitamin formulations.

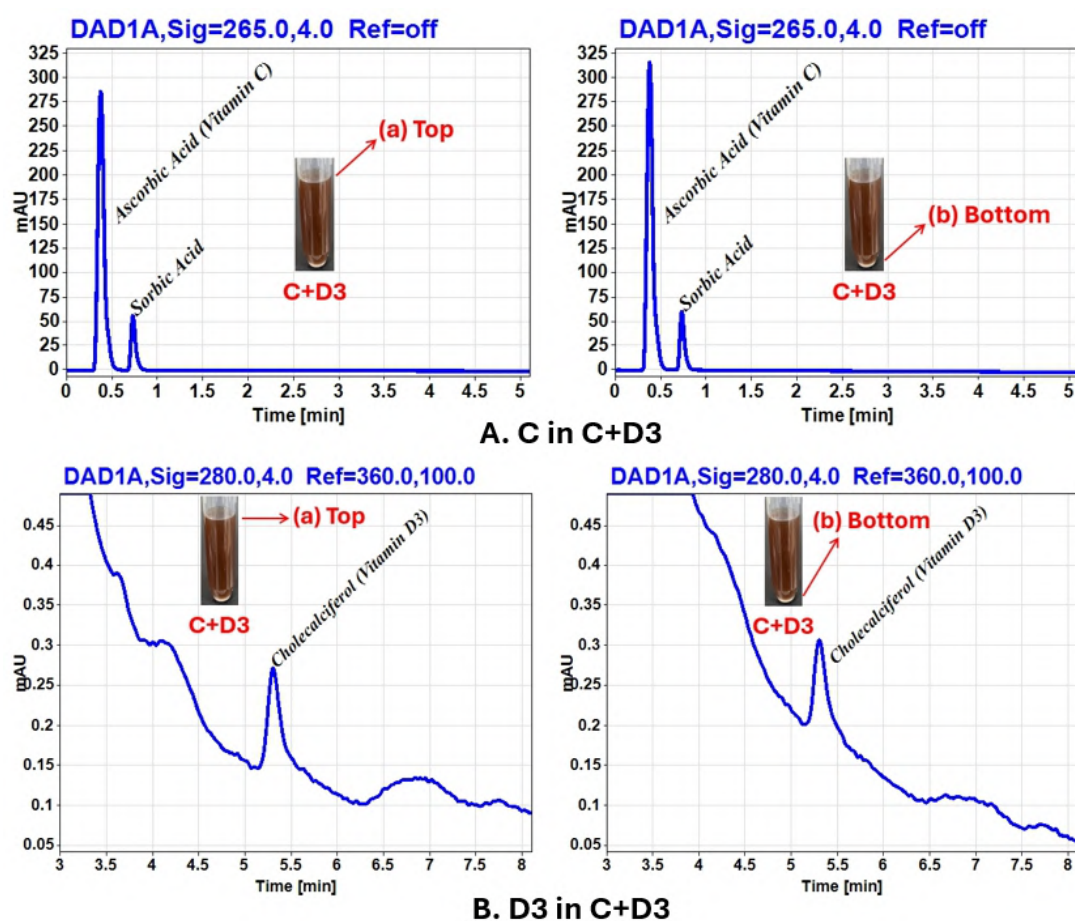


Figure 2 A. (a) A representative chromatogram of vitamin C from the top area of liposomal vitamin C plus D3. (b) A representative chromatogram of vitamin C from the bottom area of liposomal vitamin C plus D3. B. (a) A representative chromatogram of vitamin D3 from the top area of liposomal vitamin C plus D3. (b) A representative chromatogram of vitamin D3 from the bottom area of liposomal vitamin C plus D3.

Table 2 Concentrations of liposomal vitamin C plus vitamin D3 from top and bottom

Liposomal Vitamin C plus Vitamin D3	Top	Bottom
Vitamin C	Concentration 197.5 mg/mL Recovery value (%) (98.8%)	203.3 mg/mL (101.6%)
Vitamin D3	Concentration 5.13 μ g/mL Recovery value (%) (102.5%)	4.77 μ g/mL (95.3%)

The concentrations of liposomal vitamin VC plus vitamin VD3 from both the upper and lower layers are shown in the inset. The two separate sample regions are labelled as Top (a) and Bottom (b).

3.6 Determination of calcium and vitamin D3 potencies in liposomal calcium and liposomal calcium plus vitamin D3

The calcium and vitamin D3 potencies in both the water-based and lipid-based formulations of liposomal calcium and liposomal calcium plus vitamin D3 were determined using ultrahigh-performance liquid chromatography (UHPLC) equipped with a DAD detector at wavelengths of 195 nm for L-aspartic acid and 280 nm for vitamin D3. Table 3 shows the calcium and VD3 concentrations in the top and lower areas of the sample tube (see inset images in Figures 3A. a-b, 3B. a-b, and 3C. a-b). The calcium recovery (%) was 106.7% and 113.1%, whereas the VD3 recovery (%) was 95.6% and 86.3%. Furthermore, the calcium concentrations levels in the

top and lower portions of the liposomal calcium were 98.8% and 103.3%, respectively. Based on these observations, it was established that the sample was visibly uniform and did not exhibit any notable phase separation. In accordance with the regulations set by Health Canada for Natural Health Products, a permissible variation in composition of up to 20% is acceptable, as indicated in 3.5.

Table 3 Concentrations of liposomal calcium plus vitamin D3 and liposomal calcium from top and bottom

Liposomal Calcium plus	Vitamin D3	Top	Bottom
Vitamin D3	Concentration	2.39 $\mu\text{g}/\text{mL}$	2.16 $\mu\text{g}/\text{mL}$
	Recovery value (%)	(95.6%)	(86.3%)
Calcium L-Aspartate	Concentration	106.7 mg/mL	113.1 mg/mL
	Recovery value (%)	(98.4%)	(104.3%)
Liposomal Calcium		Top	Bottom
Calcium L-Aspartate	Concentration	142.8 mg/mL	149.3 mg/mL
	Recovery value (%)	(98.8%)	(103.3%)

The inset shows the concentrations of liposomal calcium plus vitamin D3 and liposomal calcium from both the upper and lower layers, which includes two distinct sample regions labeled as Top (a) and Bottom (b). The core objective of co-encapsulating both calcium L-aspartate and vitamin D3 within a single liposomal formulation is to synergistically enhance the bioavailability of these vital nutrients. This is particularly significant considering that highly water-soluble calcium species can readily traverse cellular membranes via dedicated calcium-permeable ion channels (Catterall, 2011), whereas liposomal encapsulation offers a more effective mechanism for the delivery of vitamin D3 into target cells (Cooper and Dimri, 2021).

3.7 Comparison of Vitamin and Mineral Formulations

The colloidal size of developed bioactive formulations plays a crucial role in influencing their stability, biophysical activity, and overall effectiveness (Zhao et al., 2017; Mozafari et al., 2008). The particle sizes of liposomal vitamin C and vitamin D3 were compared in this study, and they were found to have similar sizes (100-200 nm) to those predicted for individual liposomal vitamin C (200 nm) and individual liposomal vitamin D3 (100 nm) (Chen et al., 2022). However, the particle size of liposomal calcium plus vitamin D3 has a wider size range (50-800 nm) than that of individual liposomal calcium (100-300 nm), which could be due to the favorable hydration of calcium ions. Indeed, increasing the absolute zeta potential could lead to significant alterations in particle size (Nsairat et al., 2022).

In general, for the three formulations studied, the concentration of the upper and lower regions of the liposomal liquid did not show any significant difference in the composition of the vitamin levels, indicating the homogeneity of these liposome formulations.

3.8 Stability

The composition of the various liposome formulations remained stable at 4 °C and 25 °C after 6 months. Calcium L-aspartate was the most stable compound during longer-term stability and throughout the simulated digestion testing. Vitamin C may have undergone some degradation due to oxidation, whereas vitamin D3 was the least stable formulation.

The findings of this study, presented in Tables 4-6, indicate that the liposomal formulations containing entrapped vitamins exhibited minimal leakage over a 6-month duration, both at 4°C and 25 °C, when compared to the samples evaluated immediately after the liposomal preparation.

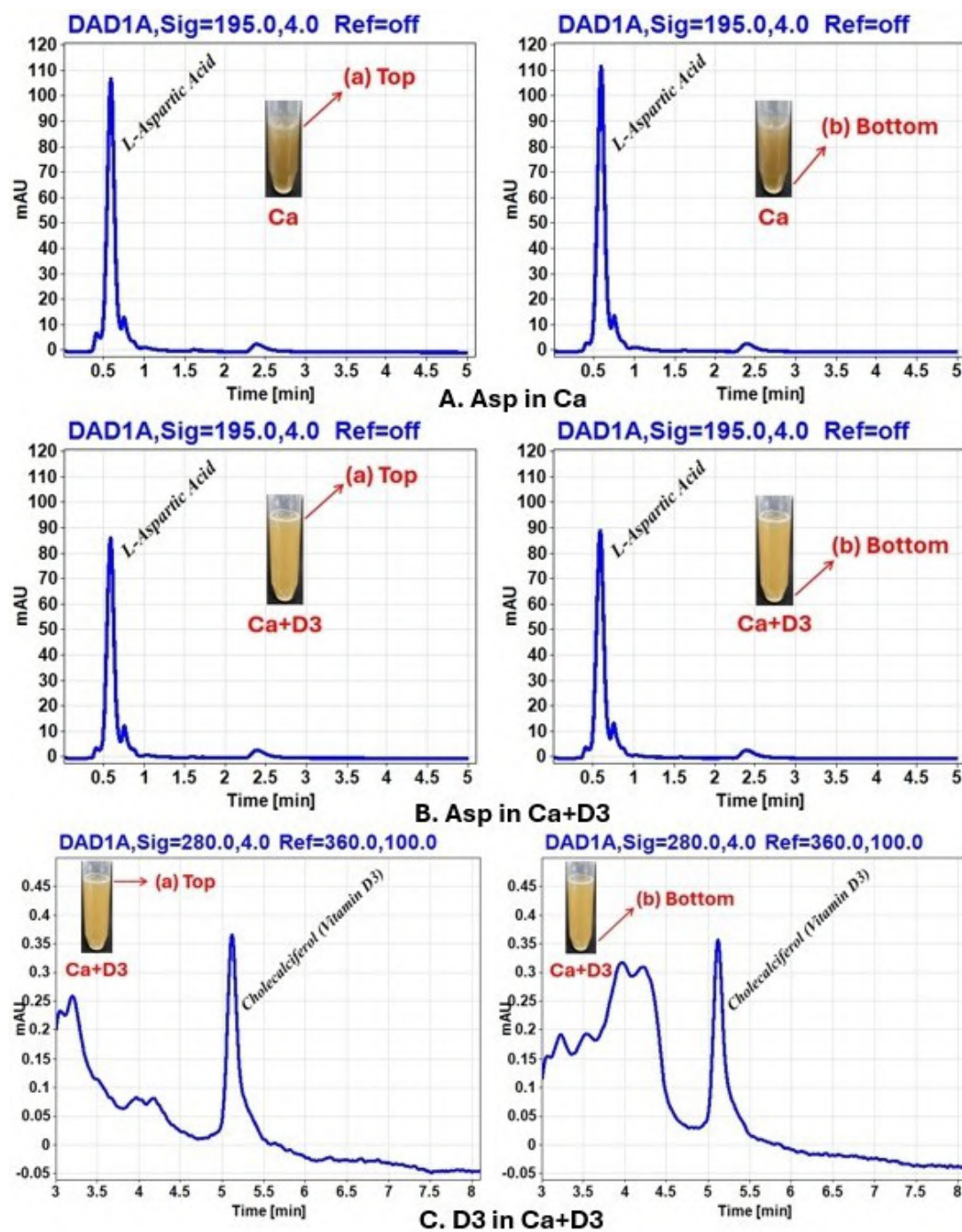


Figure 3 A. (a) Representative chromatogram of calcium L-aspartate from the top region of liposomal calcium. (b) Representative chromatogram of calcium L-aspartate from the bottom region of liposomal calcium. B. (a) Representative chromatogram of calcium L-aspartate from the top region of liposomal calcium plus D3. (b) Representative chromatogram of calcium L-aspartate from the bottom region of liposomal calcium plus D3. C. (a) A representative chromatogram of vitamin D3 from the top section of liposomal calcium plus D3, and (b) A representative chromatogram of vitamin D3 from the bottom region of liposomal calcium plus D3

3.9 In vitro stability of digestion

As shown in Figure 4, the stability of vitamin C and vitamin D3 gradually decreased within 6 months and through simulated gastric and intestinal system possibly due to oxidation and pH variations caused degradation (Shofinita et al., 2025). On the contrary, the concentration of

calcium L-aspartate in both liposomal calcium plus VD3 and liposomal calcium was very stable without almost any change in conditions. Similar to stability, the EE (%) for vitamin C and vitamin D3 decreased with time and through the simulated digestive system (Figure 5). Vitamin D3 has a relatively high EE% in both liposomal vitamin C plus vitamin D3 and liposomal calcium plus vitamin D3. The trend of vitamin loading (VL%) was consistent with EE in both formulations. The EE% and VL% of calcium L-aspartate were not quantitatively determined due to experimental uncertainties in the results because the level of calcium encapsulation was not clear by the preparation method employed here. In addition, the combination of calcium and vitamin D3 revealed good stability throughout the digestive system. In contrast to labile vitamins, encapsulating calcium by liposomes is not necessary because it can be transported through cell membranes via ion channels. Unlike vitamin D3, which is lipid-soluble and cannot directly pass through the cellular membrane, liposomal encapsulated forms facilitate transport into the cell.

Table 4 Stability of liposomal vitamin C plus vitamin D3 under storage at 4 °C and 25 °C

Liposomal Vitamin C plus Vitamin D3	Storage Temperature (°C)	0 Days		180 Days	
		Top	Bottom	Top	Bottom
Concentration of Vitamin C	4	197.5 mg/mL	203.3 mg/mL	197.1 mg/mL	188.2 mg/mL
	25	197.5 mg/mL	203.3 mg/mL	195.1 mg/mL	184.8 mg/mL
Stability (%) of Vitamin C	4	98.8%	101.6%	98.6%	94.1%
	25	98.8%	101.6%	97.6%	92.4%
Concentration of Vitamin D3	4	5.13 µg/mL	4.77 µg/mL	4.36 µg/mL	3.77 µg/mL
	25	5.13 µg/mL	4.77 µg/mL	4.11 µg/mL	3.67 µg/mL
Stability (%) of Vitamin D3	4	102.5%	95.3%	87.3%	75.3%
	25	102.5%	95.3%	82.1%	73.4%

Table 5 Stability of liposomal calcium under storage at 4 °C and 25 °C

Liposomal Calcium	Storage Temperature (°C)	0 Days		180 Days	
		Top	Bottom	Top	Bottom
Concentration of Calcium	4	142.8 mg/mL	149.3 mg/mL	141.1 mg/mL	144.9 mg/mL
	25	142.8 mg/mL	149.3 mg/mL	142.0 mg/mL	146.1 mg/mL
Stability (%) of Calcium	4	98.8%	103.3%	97.7%	100.3%
	25	98.8%	103.3%	98.2%	101.1%

Table 6 Stability of liposomal calcium plus vitamin D3 under storage at 4 °C and 25 °C

Liposomal Calcium plus Vitamin D3	Storage Temperature (°C)	0 Days		180 Days	
		Top	Bottom	Top	Bottom
Concentration of Calcium	4	106.7 mg/mL	113.1 mg/mL	105.5 mg/mL	110.1 mg/mL
	25	106.7 mg/mL	113.1 mg/mL	105.9 mg/mL	111.8 mg/mL
Stability (%) of Calcium	4	98.4%	104.3%	97.3%	101.6%
	25	98.4%	104.3%	97.8%	103.1%
Concentration of Vitamin D3	4	2.39 µg/mL	2.16 µg/mL	2.26 µg/mL	1.86 µg/mL
	25	2.39 µg/mL	2.16 µg/mL	2.18 µg/mL	1.76 µg/mL
Stability (%) of Vitamin D3	4	95.6%	86.3%	90.4%	74.3%
	25	95.6%	86.3%	87.2%	70.5%

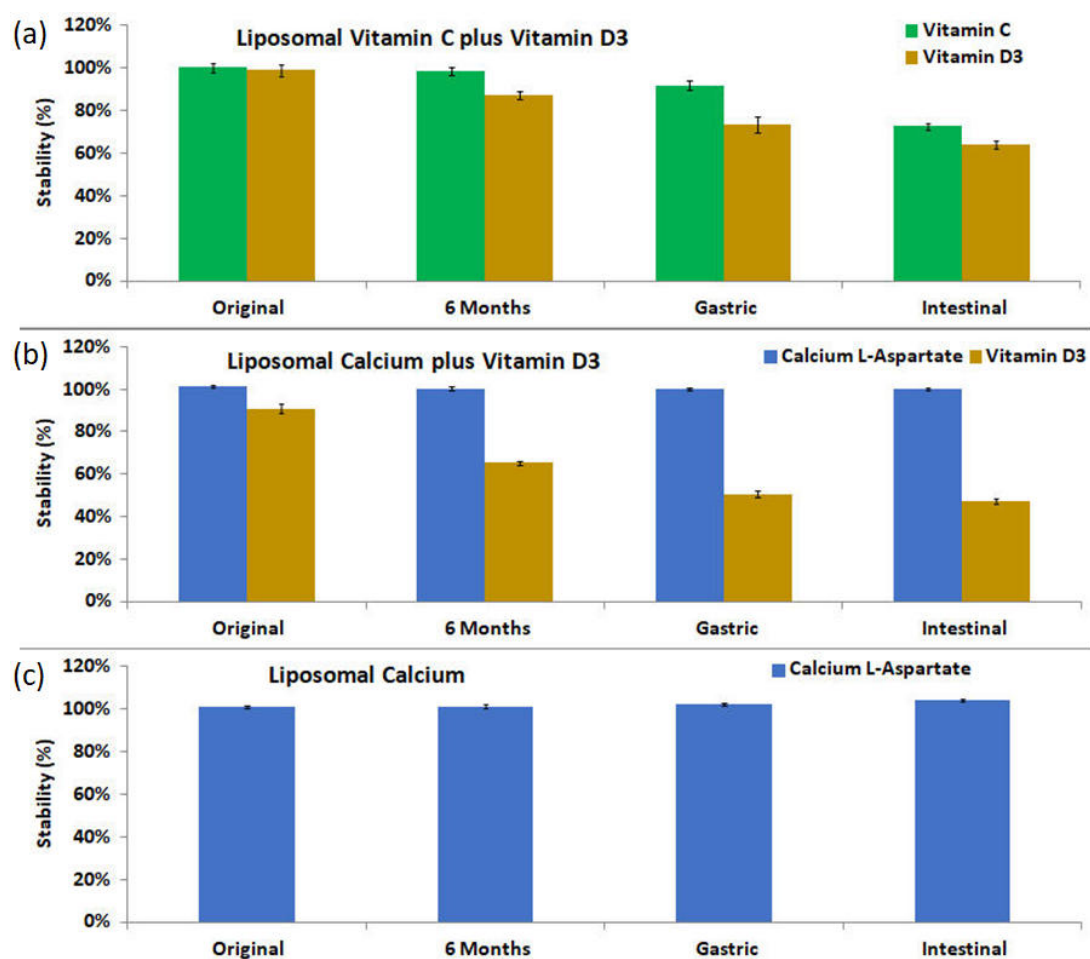


Figure 4 Comparative study for stability (%) of the original liposomal formulation, the stability (%) after 6 months at 4 °C, the stability (%) remained after incubation in simulated gastric system, and the stability (%) remained after incubation in simulated intestinal system.

(a) Stability (%) of vitamin C and vitamin D3 in liposomal vitamin C plus vitamin D3; (b) Stability (%) of calcium L-aspartate and vitamin D3 in liposomal calcium plus vitamin D3; (c) Stability (%) of calcium L-aspartate in liposomal form

The complex interaction between Ca^{2+} ions and liposomes continues to be an area of active investigation and has revealed conflicting interpretations in the literature (Skrinda-Melne et al., 2024). The intrinsic permeability of the phospholipid bilayer to hydrophilic active compounds can pose a significant challenge in achieving consistently high encapsulation efficiency in liposomal systems (Skrinda-Melne et al., 2024). Various theoretical models and experimental findings indicate that Ca^{2+} ions can interact with the phospholipid head groups, forming supersaturated regions on the bilayer surface. This phenomenon may promote the unwanted aggregation of lipid crystals (Szcześ and Sternik, 2016). In contrast, a considerable body of research suggests that a favorable interaction occurs between Ca^{2+} ions and phospholipid head groups. The binding of Ca^{2+} is believed to promote strong adsorption onto negatively charged phospholipid bilayers. Binding contributes to improved structural integrity and stability of the liposomal system (Pedersen et al., 2006). A liposomal phospholipid bilayer study found that calcium ions can induce reversible aggregation of negatively charged liposomes, which supports a mechanism distinct from irreversible membrane fusion (Melcrová et al., 2016). Although Ca^{2+} ions induce minor structural changes in phospholipids, such as increased packing density and reduced molecular mobility. At present, there are no reports that support these interactions to result in significant or damaging effects on liposomal structure (Skrinda-Melne et al., 2024). Consequently, whether calcium ions are primarily encapsulated within the liposome or are able to freely diffuse across its membrane, their presence is unlikely to compromise the encapsulation

efficiency or stability of VD3 or other critical nutrients within the liposomal formulation.

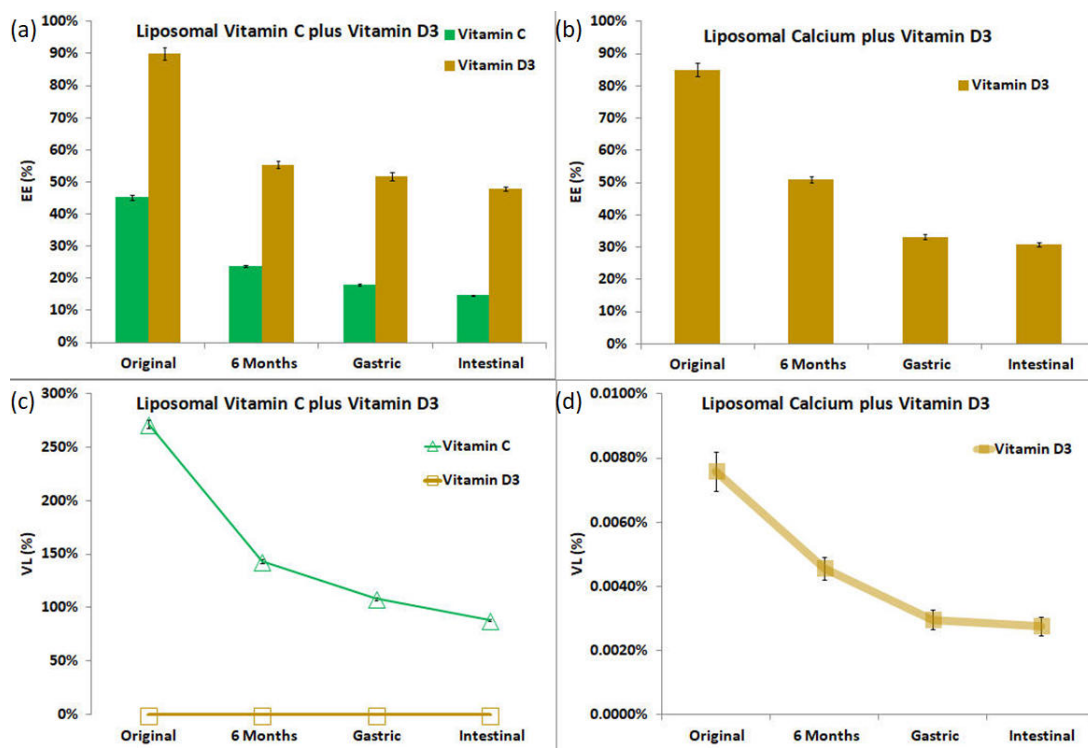


Figure 5 Comparative study for Encapsulation Efficiency (EE%) of the original liposomal formulation, the EE% after 6 months at 4 °C, the EE% remained after incubation in simulated gastric system, and the EE% remained after incubation in simulated intestinal system. (a) Encapsulation Efficiency (EE%) of vitamin C (VC) and vitamin D3 (VD3) in liposomal vitamin C plus vitamin D3; (b) Encapsulation Efficiency (EE%) of vitamin D3 in liposomal calcium plus VD3; (c) Vitamin Loading (VL%) of VC and VD3 in liposomal VC plus VD3; and (d) Vitamin Loading (VL%) of VD3 in liposomal calcium plus VD3.

Further in-depth research is needed to precisely establish the interaction between water-soluble calcium species and the liposomal membrane. Gaining insight into the interaction between water-soluble calcium species and the liposomal membrane is paramount for understanding the active and passive release profiles of these nutrients under a broad range of biologically relevant conditions (Lou and Best, 2020). The key role of Ca^{2+} in the aggregation processes of anionic biopolymers highlights the potential role of Ca^{2+} as a bridging agent (Venegas-García et al., 2024) between anionic sites of macromolecular assemblies (e.g., liposomes) and anionic cargo (e.g., VC). Further insight into the role of Ca^{2+} will involve detailed biophysical characterization using techniques such as cryo-electron microscopy, small-angle X-ray scattering, and molecular dynamics simulations to visualize and model the calcium-lipid interface at atomic resolution (Haque et al., 2024; Peter and Hubert, 2005). Furthermore, investigating the impact of varying calcium concentrations, different phospholipid compositions, and surface charge modifications on liposome integrity and cargo release kinetics will be crucial for optimizing formulation design (Yang et al., 2023). This expanded understanding will be instrumental in developing sophisticated predictive models for nutrient release in complex physiological environments, paving the way for targeted delivery strategies and personalized nutritional interventions.

4. Conclusions

The key findings of this study include a validated HPLC protocol as a robust analytical tool for the characterization of multicomponent liposomal formulations. The novel indirect quantification of calcium via L-aspartic acid chelate proved effective for assessing water-soluble calcium delivery, addressing the challenges associated with traditional inorganic calcium salts.

The formulation process yielded spherical, unilamellar vesicles with consistent particle sizes (168–329 nm). Quantitative analysis demonstrated high EE%, exceeding 90% for vitamin D3 and approximately 50% for vitamin C. Furthermore, the formulations exhibited remarkable physicochemical stability over a 6-month storage period at 4°C and 25°C, with retention rates of >98% for calcium and > 92% for vitamin C. The liposomal system provided significant protection under simulated gastrointestinal conditions, maintaining complete calcium stability and preserving the labile vitamin D3 (>30%) payload. Despite these promising results, this study has some limitations. First, although the indirect HPLC method effectively quantified total calcium, the precise encapsulation efficiency of calcium ions remains difficult to distinguish from calcium dispersed in the bulk aqueous phase due to the high permeability of the lipid bilayer to cations. The exact mechanism of calcium-membrane interaction—whether entrapped within the core or adsorbed by the phosphate head groups—requires further study. Second, bioavailability assessment was restricted to an in vitro simulated digestion model. Although this provides a useful prediction of stability, it does not fully replicate the complex sorption kinetics, first-pass metabolism, or cellular uptake mechanisms present in biological systems. Future research should prioritize two key areas: (i) advanced structural characterization techniques (e.g., cryo-electron microscopy or small-angle X-ray scattering) should be employed to visualize the atomic-level interface between calcium ions and the phospholipid bilayer, which will aid in the formulation to maximize entrapment and control release kinetics; and (ii) in vivo pharmacokinetic studies are essential to validate the clinical efficacy of these formulations. Furthermore, comparative clinical trials are needed to definitively establish whether the enhanced stability observed in vitro results translate to superior serum absorption and therapeutic bioavailability compared with non-liposomal standard-of-care supplements.

Acknowledgements

Dr. Ma's Laboratories Inc. (DML) is acknowledged for supporting this research. All liposomal samples and HPLC analyses were carried out at Dr. Ma's Laboratories Inc. L.D acknowledges Eiko Kawamura for technical support with TEM data collection at the WCVM Imaging Centre (University of Saskatchewan). L.D.W. acknowledges Deysi J. Venegas-García for technical support with zeta potential and light scattering data collection and analyses.

References

Afrooz, H., Ahmadi, F., Fallahzadeh, F., Mousavi-Fard, H., & Alipour, S. (2017). Design and characterization of paclitaxel–verapamil co-encapsulated plga nanoparticles: Potential system for overcoming p-glycoprotein mediated mdr. *Journal of Drug Delivery Science and Technology*, 41, 174–181. <https://doi.org/10.1016/j.jddst.2017.06.020>

Akbarzadeh, A., Rezaei-Sadabady, R., Davaran, S., Joo, S. W., Zarghami, N., Hanifehpour, Y., Samiei, M., Kouhi, M., & Nejati-Koshki, K. (2013). Liposome: Classification, preparation, and applications. *Nanoscale Research Letters*, 8, 102–111. <https://doi.org/10.1186/1556-276X-8-102>

AlSawaftah, N., Pitt, W. G., & Husseini, G. A. (2021). Dual-targeting and stimuli-triggered liposomal drug delivery in cancer treatment. *ACS Pharmacology & Translational Science*, 4, 1028–1049. <https://doi.org/10.1021/acsptsci.1c00066>

Barenholz, Y. C. (2012). Doxil®—the first fda-approved nano-drug: Lessons learned. *Journal of Controlled Release*, 160, 117–134. <https://doi.org/10.1016/j.jconrel.2012.03.020>

Blumberg, J. B., Cena, H., Barr, S. I., Biesalski, H. K., Dagach, R. U., Delaney, B., Frei, B., Moreno Gonzalez, M. I., Hwalla, N., Lategan-Potgieter, R., McNulty, H., Pols, J. C. V., Winichagoon, P., & Li, D. (2018). The use of multivitamin/multimineral supplements: A modified delphi consensus panel report. *Clinical Therapeutics*, 40, 640–657. <https://doi.org/10.1016/j.clinthera.2018.02.014>

Catterall, W. A. (2011). Voltage-gated calcium channels. *Cold Spring Harbor Perspectives in Biology*, 3, a003947. <https://doi.org/10.1101/cshperspect.a003947>

Chaves, M. A., Filho, P. L. O., Jange, C. G., Sinigaglia-Coimbra, R., Oliveira, C. L. P., & Pinho, S. C. (2018). Structural characterization of multilamellar liposomes coencapsulating curcumin and vitamin d3. *Colloids and Surfaces A: Physicochemical and Engineering Aspects*, 549, 112–121. <https://doi.org/10.1016/j.colsurfa.2018.04.018>

Chen, J., Dehabadi, L., Ma, Y. C., & Wilson, L. (2022). Development of novel lipid-based formulations for water-soluble vitamin c versus fat-soluble vitamin d3. *Bioengineering*, 9, 819–823. <https://doi.org/10.3390/bioengineering9120819>

Cooper, D., & Dimri, M. (2021). *Biochemistry, calcium channels*. <https://www.ncbi.nlm.nih.gov/books/NBK562198/>

Dalmoro, A., Bochicchio, S., Lamberti, G., Bertoncin, P., Janssens, B., & Barba, A. A. (2019). Micronutrients encapsulation in enhanced nanoliposomal carriers by a novel preparative technology. *RSC Advances*, 9, 19800–19812. <https://doi.org/10.1039/C9RA03022K>

Dangkoub, F., Bemani Naeini, M., Akar, S., Badiee, A., Jaafari, M. R., Sankian, M., Tafaghodi, M., & Mousavi Shaegh, S. A. (2024). Preparation of atorvastatin calcium-loaded liposomes using thin-film hydration and coaxial micromixing methods: A comparative study. *International Journal of Pharmaceutics X*, 8, 100309. <https://doi.org/10.1016/j.ijpx.2024.100309>

Daraee, H., Etemadi, A., Kouhi, M., Alimirzalu, S., & Akbarzadeh, A. (2016). Application of liposomes in medicine and drug delivery. *Artificial Cells, Nanomedicine, and Biotechnology*, 44, 381–391. <https://doi.org/10.3109/21691401.2014.953633>

Davis, J. L., Paris, H. L., Beals, J. W., Binns, S. E., Giordano, G. R., Scalzo, R. L., Schweder, M. M., Blair, E., & Bell, C. (2016). Liposomal-encapsulated ascorbic acid: Influence on vitamin c bioavailability and capacity to protect against ischemia-reperfusion injury. *Nutrition and Metabolic Insights*, 9, 25–30. <https://doi.org/10.4137/NMI.S39764>

Deshpande, P. P., Biswas, S., & Torchilin, V. P. (2013). Current trends in the use of liposomes for tumor targeting. *Nanomedicine*, 8, 1509–1528. <https://doi.org/10.2217/nnm.13.118>

Frenzel, M., Krolak, E., Wagner, A. E., & Steffen-Heins, A. (2015). Physicochemical properties of wpi coated liposomes serving as stable transporters in a real food matrix. *LWT - Food Science and Technology*, 63, 527–534. <https://doi.org/10.1016/j.lwt.2015.03.055>

Ghadami, S., & Dellinger, K. (2023). The lipid composition of extracellular vesicles: Applications in diagnostics and therapeutic delivery. *Frontiers in Molecular Biosciences*, 10. <https://doi.org/10.3389/fmbo.2023.1198044>

Haque, F., Jamali, S., & Moradi, M. (2024). Molecular dynamics simulation analysis of the effects and mechanisms of lipid nanoparticles in drug delivery systems. *Biophysical Journal*, 123, 504a. <https://doi.org/10.1016/j.bpj.2023.11.3051>

Huang, Y., Chang, Z., Gao, Y., Ren, C., Lin, Y., Zhang, X., Wu, C., Pan, X., & Huang, Z. (2024). Overcoming the low-stability bottleneck in the clinical translation of liposomal pressurized metered-dose inhalers: A shell stabilization strategy inspired by biomaterialization. *International Journal of Molecular Sciences*, 25, 3261. <https://doi.org/10.3390/ijms25063261>

Irawan, Y., Juliana, I., Adilina, I. B., & Alli, Y. (2017). Aqueous stability studies of polyethylene glycol and oleic acid-based anionic surfactants for application in enhanced oil recovery through dynamic light scattering. *International Journal of Technology*, 8(8), 1414–1421. <https://doi.org/10.14716/ijtech.v8i8.690>

Jeung, J. J. (2016). *Vitamin c delivery system and liposomal composition thereof* (US20160367480A1). <https://patents.google.com/patent/US20160367480A1/en>

Kerksick, C. M., Wilborn, C. D., Roberts, M. D., Smith-Ryan, A., Kleiner, S. M., Jäger, R., Collins, R., Cooke, M., Davis, J. N., Galvan, E., Greenwood, M., Lowery, L. M., Wildman, R., Antonio, J., & Kreider, R. B. (2018). ISSN exercise & sports nutrition review

update: Research & recommendations. *Journal of the International Society of Sports Nutrition*, 15, 38. <https://doi.org/10.1186/s12970-018-0242-y>

Ko, J., Yoo, C., Xing, D., Gonzalez, D. E., Jenkins, V., Dickerson, B., Leonard, M., Nottingham, K., Kendra, J., Sowinski, R., Rasmussen, C. J., & Kreider, R. B. (2023). Pharmacokinetic analyses of liposomal and non-liposomal multivitamin/mineral formulations. *Nutrients*, 15, 3073–3090. <https://doi.org/10.3390/nu15133073>

Kraft, J. C., Freeling, J. P., Wang, Z., & Ho, R. J. (2014). Emerging research and clinical development trends of liposome and lipid nanoparticle drug delivery systems. *Journal of Pharmaceutical Sciences*, 103, 29–52. <https://doi.org/10.1002/jps.23773>

Lee, M.-K. (2020). Liposomes for enhanced bioavailability of water-insoluble drugs: In vivo evidence and recent approaches. *Pharmaceutics*, 12(3), 264. <https://doi.org/10.3390/pharmaceutics12030264>

Liu, X., Wang, P., Zou, Y. X., Luo, Z. G., & Tamer, T. M. (2020). Co-encapsulation of vitamin c and β-carotene in liposomes: Storage stability, antioxidant activity, and in vitro gastrointestinal digestion. *Food Research International*, 136, 109587–109595. <https://doi.org/10.1016/j.foodres.2020.109587>

Lou, J., & Best, M. D. (2020). Calcium-responsive liposomes: Toward ion-mediated targeted drug delivery. *Methods in Enzymology*, 640, 105–129. <https://doi.org/10.1016/bs.mie.2020.04.005>

Lukawski, M., Dałek, P., Borowik, T., Foryś, A., Langner, M., Witkiewicz, W., & Przybyło, M. (2020). New oral liposomal vitamin c formulation: Properties and bioavailability. *Journal of Liposome Research*, 30, 227–234. <https://doi.org/10.1080/08982104.2019.1630642>

Maione-Silva, L., de Castro, E. G., Nascimento, T. L., Cintra, E. R., Moreira, L. C., Cintra, B. A. S., Valadares, M. C., & Lima, E. M. (2019). Ascorbic acid encapsulated into negatively charged liposomes exhibits increased skin permeation, retention and enhances collagen synthesis by fibroblasts. *Scientific Reports*, 9, 522. <https://doi.org/10.1038/s41598-018-36682-9>

Mankan, E., Karakas, C. Y., Saroglu, O., Mzoughi, M., Sagdic, O., & Karadag, A. (2025). Food-grade liposome-loaded delivery systems: Current trends and future perspectives. *Foods*, 14(17), 2978. <https://doi.org/10.3390/foods14172978>

Melcrová, A., Pokorna, S., Pullanchery, S., Kohagen, M., Jurkiewicz, P., Hof, M., Jungwirth, P., Cremer, P. S., & Cwiklik, L. (2016). The complex nature of calcium cation interactions with phospholipid bilayers. *Scientific Reports*, 6, 38035. <https://doi.org/10.1038/srep38035>

Mohammadi, M., Ghanbarzadeh, B., & Hamishehkar, H. (2014). Formulation of nanoliposomal vitamin d3 for potential application in beverage fortification. *Advanced Pharmaceutical Bulletin*, 4, 569–575. <https://doi.org/10.5681/apb.2014.084>

Mozafari, M. R., Johnson, C., Hatziantoniou, S., & Demetzos, C. (2008). Nanoliposomes and their applications in food nanotechnology. *Journal of Liposome Research*, 18, 309–327. <https://doi.org/10.1080/08982100802465941>

Nakhaei, P., Margiana, R., Bokov, D. O., Abdelbasset, W. K., Jadidi Kouhbanani, M. A., Varma, R. S., Marofi, F., Jarahian, M., & Beheshtkhoo, N. (2021). Liposomes: Structure, biomedical applications, and stability parameters with emphasis on cholesterol. *Frontiers in Bioengineering and Biotechnology*, 9, 705886–705909. <https://doi.org/10.3389/fbioe.2021.705886>

Noble, G. T., Stefanick, J. F., Ashley, J. D., Kiziltepe, T., & Bilgicer, B. (2014). Ligand-targeted liposome design: Challenges and fundamental considerations. *Trends in Biotechnology*, 32, 32–45. <https://doi.org/10.1016/j.tibtech.2013.09.007>

Nsairat, H., Khater, D., Sayed, U., Odeh, F., Bawab, A., & Alshaer, W. (2022). Liposomes: Structure, composition, types, and clinical applications. *Helijon*, 8, e09394. <https://doi.org/10.1016/j.helijon.2022.e09394>

Pedersen, U. R., Leidy, C., Westh, P., & Peters, G. H. (2006). The effect of calcium on the properties of charged phospholipid bilayers. *Biochimica et Biophysica Acta (BBA) - Biomembranes*, 1758, 573–582. <https://doi.org/10.1016/j.bbamem.2006.03.035>

Peter, M. F., & Hubert, D. H. W. (2005). Cryoelectron microscopy of liposomes. *Methods in Enzymology*, 391, 431–448. [https://doi.org/10.1016/S0076-6879\(05\)91024-0](https://doi.org/10.1016/S0076-6879(05)91024-0)

Raval, N., Maheshwari, R., Kalyane, D., Youngren-Ortiz, S. R., Chougule, M. B., & Tekade, R. K. (2019). Importance of physicochemical characterization of nanoparticles in pharmaceutical product development. In *Basic fundamentals of drug delivery*. Academic Press. <https://doi.org/10.1016/B978-0-12-817909-3.00010-8>

Sapei, L., Savitri, E., Jati, I. R. A., Indrawanto, R., Darsono, H. E., Anggraeni, Y., & Sumampouw, C. (2024). Stability and kinetic study of vitamin c containing hydrogenated and middle-chain triglyceride coconut oil-based double emulsion. *International Journal of Technology*, 15(6), 1982–1993. <https://doi.org/10.14716/ijtech.v15i6.6371>

Shade, C. W. (2016). Liposomes as advanced delivery systems for nutraceuticals. *Integrative Medicine*, 15(1), 33–36.

Shofinita, D., Harimawan, A., Almaishya, N., Dewi, A. M., Thamleonard, J., & Achmadi, A. B. (2025). Enhancing viability of probiotic by microencapsulation: A case study in ice cream. *International Journal of Technology*, 16(4), 1337–1347. <https://doi.org/10.14716/ijtech.v16i4.6886>

Skrinda-Melne, M., Locs, J., Grava, A., & Dubnika, A. (2024). Calcium phosphates enhanced with liposomes - the future of bone regeneration and drug delivery. *Journal of Liposome Research*, 34(3), 507–522. <https://doi.org/10.1080/08982104.2023.2285973>

Strange, R. C., Shipman, K. E., & Ramachandran, S. (2015). Metabolic syndrome: A review of the role of vitamin d in mediating susceptibility and outcome. *World Journal of Diabetes*, 6, 896–911. <https://doi.org/10.4239/wjd.v6.i7.896>

Szczęś, A., & Sternik, D. (2016). Properties of calcium carbonate precipitated in the presence of dppc liposomes modified with the phospholipase a2. *Journal of Thermal Analysis and Calorimetry*, 123, 2357–2365. <https://doi.org/10.1007/s10973-015-4958-5>

Tenchov, R., Bird, R., Curtze, A. E., & Zhou, Q. (2021). Lipid nanoparticles-from liposomes to mrna vaccine delivery, a landscape of research diversity and advancement. *ACS Nano*, 15, 16982–17015. <https://doi.org/10.1021/acsnano.1c04996>

Tinsley, G. M., Harty, P. S., Stratton, M. T., Siedler, M. R., & Rodriguez, C. (2022). Liposomal mineral absorption: A randomized crossover trial. *Nutrients*, 14, 3321–3337. <https://doi.org/10.3390/nu14163321>

US Preventive Services Task Force, Mangione, C. M., Barry, M. J., Nicholson, W. K., Cabana, M., Chelmow, D., Coker, T. R., Davis, E. M., Donahue, K. E., Doubeni, C. A., Jaen, C. R., Kubik, M., Li, L., Ogedegbe, G., Pbert, L., Ruiz, J. M., Stevermer, J., & Wong, J. B. (2022). Vitamin, mineral, and multivitamin supplementation to prevent cardiovascular disease and cancer: Us preventive services task force recommendation statement. *JAMA*, 327, 2326–2333. <https://doi.org/10.1001/jama.2022.8970>

Vakilnezhad, M. A., Amini, A., Akbari-Javar, H., Bahā'addini Beigi Zarandi, B. F., Montaseri, H., & Dinarvand, R. (2018). Nicotinamide loaded functionalized solid lipid nanoparticles improves cognition in alzheimer's disease animal model by reducing tau hyperphosphorylation. *DARU Journal of Pharmaceutical Sciences*, 26, 165–177. <https://doi.org/10.1007/s40199-018-0221-5>

Venegas-García, D. J., D, W. L., & Cruz-Guzmán, M. D. l. (2024). Aloe vera mucilage as a sustainable biopolymer flocculant for efficient arsenate anion removal from water. *RSC Sustainability*, 2(9), 2632–2643. <https://doi.org/10.1039/d4su00170b>

Wibowo, A., Jatmiko, A., Ananda, M. B., Rachmawati, S. A., Ardy, H., Aimon, A. H., & Iskandar, F. (2021). Facile fabrication of polyelectrolyte complex nanoparticles based on chitosan–poly-2-acrylamido-2-methylpropane sulfonic acid as a potential drug carrier

material. *International Journal of Technology*, 12(3), 561–570. <https://doi.org/10.14716/ijtech.v12i3.4193>

Yang, K., Tran, K., & Salvati, A. (2023). Tuning liposome stability in biological environments and intracellular drug release kinetics. *Biomolecules*, 13, 59. <https://doi.org/10.3390/biom13010059>

Zhao, L., Temelli, F., & Chen, L. (2017). Encapsulation of anthocyanin in liposomes using supercritical carbon dioxide: Effects of anthocyanin and sterol concentrations. *Journal of Functional Foods*, 34, 159–167. <https://doi.org/10.1016/j.jff.2017.04.021>